NASA TECHNICAL NOTE

NASA TN D-7447

NASA TN D-7447

EFFECT OF GEOMETRY VARIATIONS ON LEE-SURFACE VORTEX-INDUCED HEATING FOR FLAT-BOTTOM THREE-DIMENSIONAL BODIES AT MACH 6

by Jerry N. Hefner

Langley Research Center
Hampton, Va. 23665

NATIONAL AERONAUTICS AND SPACE ADMINISTRATION • WASHINGTON, D. C. • NOVEMBER 1973

1. Report No.	2. Government Accession No.	3. Recipient's Catalog No.
NASA TN D-7447		

4. Title and Subtitle	5. Report Date
EFFECT OF GEOMETRY VARIATIONS ON LEE-SURFACE VORTEX-INDUCED HEATING FOR FLAT-BOTTOM THREE-DIMENSIONAL BODIES AT MACH 6	November 1973
	6. Performing Organization Code

7. Author(s)	8. Performing Organization Report No.
Jerry N. Hefner	L-9209
	10. Work Unit No. 502-37-01-11
9. Performing Organization Name and Address	11. Contract or Grant No.
NASA Langley Research Center Hampton, Va. 23665	
	13. Type of Report and Period Covered
12. Sponsoring Agency Name and Address	Technical Note
National Aeronautics and Space Administration Washington, D.C. 20546	14. Sponsoring Agency Code

15. Supplementary Notes

16. Abstract

Recent experimental studies have shown that vortices can produce relatively severe heating on the leeward surfaces of conceptual hypersonic vehicles and that surface geometry can strongly influence this vortex-induced heating. This paper presents experimental results which show the effects of systematic geometry variations on the vortex-induced lee-surface heating on simple flat-bottom three-dimensional bodies at angles of attack of 20° and 40°. The tests were conducted at a free-stream Mach number of 6 and at a Reynolds number of 1.71×10^{7} per meter.

17. Key Words (Suggested by Author(s))	18. Distribution Statement
Heat transfer Lee surface Angle of attack Three-dimensional bodies Geometry variations	Unclassified – Unlimited

19. Security Classif. (of this report)	20. Security Classif. (of this page)	21. No. of Pages	22. Price*
Unclassified	Unclassified	28	Domestic, $3.00 Foreign, $5.50

*For sale by the National Technical Information Service, Springfield, Virginia 22151

EFFECT OF GEOMETRY VARIATIONS ON LEE-SURFACE VORTEX-INDUCED HEATING FOR FLAT-BOTTOM THREE-DIMENSIONAL BODIES AT MACH 6

By Jerry N. Hefner
Langley Research Center

SUMMARY

The effects of systematic geometry variations on the lee-surface vortex-induced heating for simple flat-bottom three-dimensional bodies at angles of attack of 20° and 40° at Mach 6 are presented. Relatively high levels of vortex-induced heating were found on the lee surfaces of each body since none of the geometry variations entirely eliminated the adverse heating effects of the vortices. Secondary vortices were generated as a result of blunting the chine radius and/or increasing the angle of attack. Vortices were also generated on the sides of the afterbody at the abrupt change in planform area (surface discontinuity between model forebody and afterbody). The secondary and side vortices were found to produce levels of heating that could be equal to or greater than that produced by the primary vortices; thereby, the expected favorable effects of the surface discontinuity would be nullified. Reducing nose bluntness to obtain a sharp nose body significantly increased the vortex-induced heating on the forebody lee meridian.

INTRODUCTION

Recent experimental studies have shown that vortices strongly influence heating on the leeward surface of conceptual hypersonic vehicles. (See refs. 1 to 6.) Some of the significant conclusions from these studies include (1) peak vortex-induced lee-surface heating at an angle of attack can exceed that for zero angle of attack; (2) peak heating is extremely sensitive to Reynolds numbers; (3) a "threshold" Reynolds number exists below which peak vortex-induced heating decreases abruptly; (4) lee-surface vortex flow modeling differs from conventional separation flow modeling; and (5) the geometry of the lee surface greatly influences the vortical heating for three-dimensional configurations. Although the studies showing the influence of lee-surface geometry on the vortical heating provides some information which was used to control partially the severity of the lee-surface heating, more refined guidelines on vortex alleviation are needed. Therefore, experimental data are necessary to define better the relationship between the lee-surface

geometry and the resulting leeward flow field and surface heat transfer. Information of this type is available for planar delta wings, but is nonexistent for three-dimensional geometries.

This paper presents experimental results which show the effects of systematic geometry variations on the lee-surface vortex-induced heating for simple flat-bottom three-dimensional bodies. The study was conducted in conjunction with the investigation reported in references 1 to 3. The tests were conducted at a free-stream Mach number of 6 and at a free-stream Reynolds number of 1.71×10^7 per meter.

SYMBOLS

h	local heat-transfer coefficient
h_{ref}	stagnation heat-transfer coefficient on a 0.305-m (1-foot) radius sphere scaled by the same factor as the wind-tunnel model
L	model length
M_∞	free-stream Mach number
$R_{\infty,L}$	free-stream Reynolds number based on model length
s	longitudinal surface distance measured from model nose
x	longitudinal coordinate of body measured from model nose
y	local half-width of body
α	angle of attack

Subscripts:

1	conditions at position of first vortex-induced lee-surface heating peak
2	conditions at position of second vortex-induced lee-surface heating peak

APPARATUS AND METHODS

Tunnel

This experiment was conducted in the Langley 20-inch Mach 6 tunnel. A complete description of this tunnel and its calibration is given in the appendix of reference 7.

Models and Test Conditions

Six flat-bottom models with various forebody shapes were used; sketches of these models are given in figure 1. The geometry variations selected were those that were believed to have the most effect on the vortex-induced heating. All models incorporated a surface discontinuity between the forebody and afterbody which was intended to induce the vortices to lift off the surface at the discontinuity. (See ref. 3.) The models were made of a mica-stycast resin. The thermophysical properties of this material were measured from samples cast at the same time as the models.

Tests were conducted at a free-stream Reynolds number of 1.71×10^7 per meter. The total temperature was 497 K, and the ratio of wall temperature to total temperature was approximately 0.6. The angles of attack were 20° and 40°.

Test Methods

Heat-transfer data were obtained by using the phase-change-paint technique (ref. 8) and were recorded on 35-mm motion-picture film at the rate of 10 frames per second. A network of grid lines spaced 1.27 cm apart and measured longitudinally from the rear of the model was used to locate the line of constant heating. The grid lines on either side of the top meridian on the model were also 1.27 cm apart on the model afterbody, the grid spacing being proportionately smaller as the distance from the model nose on the forebody is decreased. Phase-change paints which permitted the data to be obtained within test times of approximately 20 seconds were selected. An analysis of the thermal diffusion through the mica-stycast material indicated that this time would keep conduction errors to a minimum.

Oil-flow studies were conducted to examine the surface flow and separation boundaries on the upper surfaces. A mixture of silicon oil and lampblack was distributed in random dots of varying sizes over the entire upper surface. Photographs were then taken of the models after each test. No oil-flow studies were obtained on model 2 since it was destroyed during the tunnel shutdown following the heating studies.

Data Reduction

The heat-transfer data were reduced to local heat-transfer coefficients by the method of reference 8. Since recovery factors for lee-side flow are unknown, the present data were reduced by assuming a laminar recovery factor of 0.86 based on free-stream conditions. The local heat-transfer coefficient was normalized by the calculated stagnation heat-transfer coefficient by the method of Fay and Riddell (ref. 9), on a sphere having a 0.305-m (1-foot) radius scaled by the same factor as the model at the same test

conditions. The model scale used in the reduction of the data was selected to be 0.0106 so that the data would be compatible with those presented in references 1 to 3.

RESULTS AND DISCUSSION

General Surface Flow and Heat-Transfer Characteristics

Oil-flow studies on the flat-bottom bodies at angle of attack show a highly complex lee-surface flow containing a number of vortices. The schematic drawing of figure 2 was developed with the aid of these oil-flow studies and identifies many characteristics of the lee-surface flow. On the forebody of the models, upstream of the surface discontinuity, the windward flow expands around to the leeward (shielded) surface and remains attached for a finite distance before it separates and forms a vortex. This primary vortex scrubs the lee surface in the vicinity of the lee meridian. (The scrubbing action of vortices is indicated by featherlike oil smears.) Under some conditions, secondary vortices, which are smaller in size than the primary vortices, are formed outboard of the primary vortices. (See schematic drawing of fig. 2.) These secondary vortices not only interact with the forebody lee surface, but also may interact with the afterbody surface. In addition to both the primary and secondary vortices, vortices are generated on the sides of the leeward afterbody at the abrupt change in planform area (surface discontinuity between forebody and afterbody) near the windward surface.

A comparison of the heating distributions and oil-flow patterns presented in figures 3 and 4 shows, as was found in references 1 to 3, that relatively high or elevated heating generally accompanied the interaction of vortices with the leeward surfaces, whereas lower heating accompanied separation and low surface shear. The number of vortex-induced heating peaks along the forebody lee meridian (other than the stagnation heating peaks on the nose) increased with angle of attack. The first of these heating peaks was always the maximum and was caused by the primary vortices thinning the viscous layer on the lee surface to a minimum; thereby the insulating layer between the high energy inviscid flow and the surface was reduced. (See ref. 6.)

Effect of Geometry Variations

The baseline configuration is represented by the blunted half-cone body (model 1) and the data generated on it are shown in figures 3(a) and 4(a). Results obtained on the other bodies show the effects of increasing chine radius (model 2, figs. 3(b) and 4(b)), increasing cone half-angle (model 3, figs. 3(c) and 4(c)), reducing cross-sectional area (model 4, figs. 3(d) and 4(d)), reshaping forebody to increase planform area (model 5, figs. 3(e) and 4(e)), and reducing nose bluntness (model 6, figs. 3(f) and 4(f)). Table I

provides a summary of the vortex-induced peak heating along the forebody lee meridian for all geometry variations.

Baseline configuration.- Moderately high heating is generated on the forebody lee meridian by the primary vortices at $\alpha = 20^{\circ}$. At $\alpha = 40^{\circ}$, two vortex-induced heating peaks are generated along the forebody lee meridian with the first of these nearly 50 percent higher than the single heating peak at $\alpha = 20^{\circ}$. Secondary vortices are formed on the forebody outboard of the primary vortices only at $\alpha = 40^{\circ}$, and these vortices produce regions of elevated heating on both the forebody and afterbody. On the afterbody at $\alpha = 20^{\circ}$, the side-generated vortices produce heating that is twice as high as the vortex-induced heating on the forebody. This heating, produced by the side-generated vortices, is affected only slightly by increasing the angle of attack from 20° to 40°.

Effect of increasing the chine radius.- The effect of increasing the chine radius is seen by comparing the results for model 2 with those for model 1. (See table I and compare figs. 3(b) and 4(b) with figs. 3(a) and 4(a).) Blunting the chine radius almost doubled the level of the single vortex-induced heating peak on the forebody at $\alpha = 20^{\circ}$ but only slightly affected the levels of the first and second vortex-induced heating peaks on the forebody at $\alpha = 40^{\circ}$. Furthermore, secondary vortices are produced by blunting the chine radius at both $\alpha = 20^{\circ}$ and $\alpha = 40^{\circ}$ and these vortices interact with the forebody and afterbody lee surfaces to produce elevated heating levels. The side-generated vortices produce elevated levels of heating which are lower than those found on model 1 at the same angles of attack.

Effect of increasing the cone half-angle.- The effect of increasing the cone half-angle is seen by comparing the results for model 3 with those for model 2. (See table I and compare figs. 3(c) and 4(c) with figs. 3(b) and 4(b).) Increasing the cone half-angle eliminated the formation of vortices on the forebody at $\alpha = 20^{\circ}$, but increased the single vortex-induced heating on the forebody at $\alpha = 40^{\circ}$ by 31 percent. On the afterbody at $\alpha = 20^{\circ}$, the secondary and side vortex-induced heating levels are greater than those for the primary vortices even though a large well-defined featherlike oil smear was generated by the primary vortices along the afterbody lee meridian. This result is in contrast to that reported in references 1 to 3 and 6 where the most severe vortex-induced heating was always generated by the primary vortices along the lee meridian. Therefore, the presence of a well-defined featherlike oil smear on the lee meridian should not necessarily be interpreted as the region of most severe vortex-induced heating. Also, it appears that shaping a configuration to alleviate only the effects of the primary vortices can cause some potentially serious heating problems, since the secondary and side vortices can produce heating levels equal to or greater than those produced by the primary vortices. At $\alpha = 40^{\circ}$, however, the primary vortex-induced heating peak along the

forebody lee meridian is again significantly higher than the heating levels generated by either the secondary or side vortices.

Effect of decreasing the cross-sectional area.- The effect of decreasing the cross-sectional area is seen by comparing the results for model 4 with those for model 2. (See table I and compare figs. 3(d) and 4(d) with figs. 3(b) and 4(b).) Decreasing the cross-sectional area decreases the single vortex-induced heating peak along the forebody lee meridian at $\alpha = 20^{\circ}$, but substantially increases the magnitude of the first and second vortex-induced heating peaks on the forebody lee meridian at $\alpha = 40^{\circ}$. Side-generated vortices produce heating levels on the afterbody at $\alpha = 20^{\circ}$ comparable with that produced by the primary vortices on the forebody. However, at $\alpha = 40^{\circ}$, the interaction of the side-generated vortices with the afterbody surface is apparently eliminated.

Effect of increasing planform area.- The effect of increasing planform area can be seen by comparing the results for model 5 with those for models 3 and 4. (See table I and compare figs. 3(e) and 4(e) with figs. 3(c) and 3(d) and figs. 4(c) and 4(d).) Increasing the planform area and the slope of the forebody lee meridian, as well as decreasing the cross-sectional area (the geometry variations included on model 5), eliminated the vortices on the forebody lee surface at $\alpha = 20^{\circ}$ and slightly decreased the single vortex-induced heating peak on the forebody lee meridian at $\alpha = 40^{\circ}$. The elimination of the vortices on the forebody can be attributed to the increased slope of the forebody lee meridian and agrees with the results obtained for increasing the cone half-angle (model 3). The slight decrease in the level of the single heating peak on the forebody of model 5 at $\alpha = 40^{\circ}$ can be attributed to the change in planform area since increasing the slope of the forebody lee meridian and decreasing the cross-sectional area (model 4 compared with model 2) was found to increase the vortex-induced heating peaks at $\alpha = 40^{\circ}$. As was also found for model 3 at $\alpha = 20^{\circ}$, the heating caused by the secondary and side vortices on the afterbody lee surface exceeds that for the primary vortices on the afterbody. Afterbody heating of this type somewhat nullifies the expected favorable effects of the surface discontinuity found in reference 3. At $\alpha = 40^{\circ}$, the effects of the side vortices on the afterbody are eliminated probably because of the reduced cross-sectional area.

Effect of reducing nose bluntness.- The effect of reducing nose bluntness can be seen by comparing the results for model 6 with those of model 1. (See table I and compare figs. 3(f) and 4(f) with figs. 3(a) and 4(a).) Reducing the nose bluntness of model 1 to obtain the sharp nose model 6 significantly increased the peak vortex-induced heating on the forebody at $\alpha = 20^{\circ}$ and 40°. The data of reference 3 indicated that for blunt-nose configurations (bluntnesses similar to that of model 1) doubling the nose bluntness had little effect on the level of the vortex-induced heating even though it did influence the "threshold" Reynolds number. Therefore, the level of vortex-induced heating can be reduced significantly by avoiding sharp nose bodies.

CONCLUDING REMARKS

The effects of systematic geometry variations on the lee-surface vortex-induced heating for simple flat-bottom three-dimensional bodies at angles of attack of 20° and 40° at Mach 6 have been presented. Each model incorporated a surface discontinuity which was intended to induce the primary vortices to lift off the surface at the discontinuity. Relatively high levels of vortex-induced heating were found on the lee surfaces of each configuration since none of the geometry variations entirely eliminated the adverse heating effects of the vortices. Secondary vortices, smaller in size than the primary vortices, were generated by blunting the chine radius and/or increasing the angle of attack. Vortices were also generated on the sides of the afterbody at the abrupt change in planform area (surface discontinuity between the model forebody and afterbody) near the windward surface. Increasing the cone half-angle and/or increasing the planform area of the forebody caused the levels of heating produced by the secondary and side vortices to exceed that produced by the primary vortices on the afterbody; thereby, the expected favorable effects of the surface discontinuity were nullified. Since the secondary and side vortices can produce heating levels equal to or greater than those produced by the primary vortices, potentially serious heating problems might be encountered if a configuration is shaped to alleviate only the effects of the primary vortices. Decreasing the cross-sectional area eliminated the effects of the side vortices on the afterbody at $\alpha = 40^{\circ}$. Reducing the nose bluntness to obtain a sharp-nose body significantly increased the vortex-induced heating on the forebody lee meridian.

Langley Research Center,
National Aeronautics and Space Administration,
Hampton, Va., September 21, 1973.

REFERENCES

1. Hefner, Jerry N.; and Whitehead, Allen H., Jr.: Lee-Side Heating Investigations. Pt. I – Experimental Lee-Side Heating Studies on a Delta-Wing Orbiter. NASA Space Shuttle Technology Conference. NASA TM X-2272, 1971, pp. 267-287.

2. Hefner, Jerry N.; and Whitehead, Allen H., Jr.: Lee-Side Flow Phenomena on Space Shuttle Configurations at Hypersonic Speeds. Pt. II – Studies of Lee-Surface Heating at Hypersonic Mach Numbers. Space Shuttle Aerothermodynamics Technology Conference, Vol. II. NASA TM X-2507, 1972, pp. 451-467.

3. Hefner, Jerry N.: Lee-Surface Heating and Flow Phenomena on Space Shuttle Orbiters at Large Angles of Attack and Hypersonic Speeds. NASA TN D-7088, 1972.

4. Connor, L. E.: Heat Transfer Tests of the Lockheed Space Shuttle Orbiter Configuration Conducted at the Langley Research Center Mach 8 Variable Density Tunnel. TM 54/20-241, Lockheed Missiles & Space Co., Dec. 1969.

5. Lockman, William K.; and DeRose, Charles E.: Aerodynamic Heating of a Space Shuttle Delta-Wing Orbiter. NASA TM X-62057, 1971.

6. Whitehead, Allen H., Jr.; Hefner, Jerry N.; and Rao, D. M.: Lee-Surface Vortex Effects Over Configurations in Hypersonic Flow. AIAA Paper No. 72-77, Jan. 1972.

7. Goldberg, Theodore J.; and Hefner, Jerry N. (With appendix by James C. Emery): Starting Phenomena for Hypersonic Inlets With Thick Turbulent Boundary Layers at Mach 6. NASA TN D-6280, 1971.

8. Jones, Robert A.; and Hunt, James L.: Use of Fusible Temperature Indicators for Obtaining Quantitative Heat-Transfer Data. NASA TR R-230, 1966.

9. Fay, J. A.; and Riddell, F. R.: Theory of Stagnation Point Heat Transfer in Dissociated Air. J. Aeronaut. Sci., vol. 25, no. 2, Feb. 1958, pp. 73-85, 121.

TABLE I.- LOCATION AND MAGNITUDE OF VORTEX-INDUCED PEAK HEATING ALONG FOREBODY LEE MERIDIAN

Model	α, deg	s_1/L	h_1/h_{ref}	s_2/L	h_2/h_{ref}
1	20	0.47	0.065	----	-----
2	20	.47	.125	----	-----
3	20	----	-----	----	-----
4	20	.51	.080	----	-----
5	20	----	-----	----	-----
6	20	.15	.200	----	-----
1	40	.17	.094	0.44	0.062
2	40	.15	.107	.48	.054
3	40	.27	.140	----	-----
4	40	.18	.142	.32	.102
5	40	.30	.125	----	-----
6	40	.07	.163	.35	.070

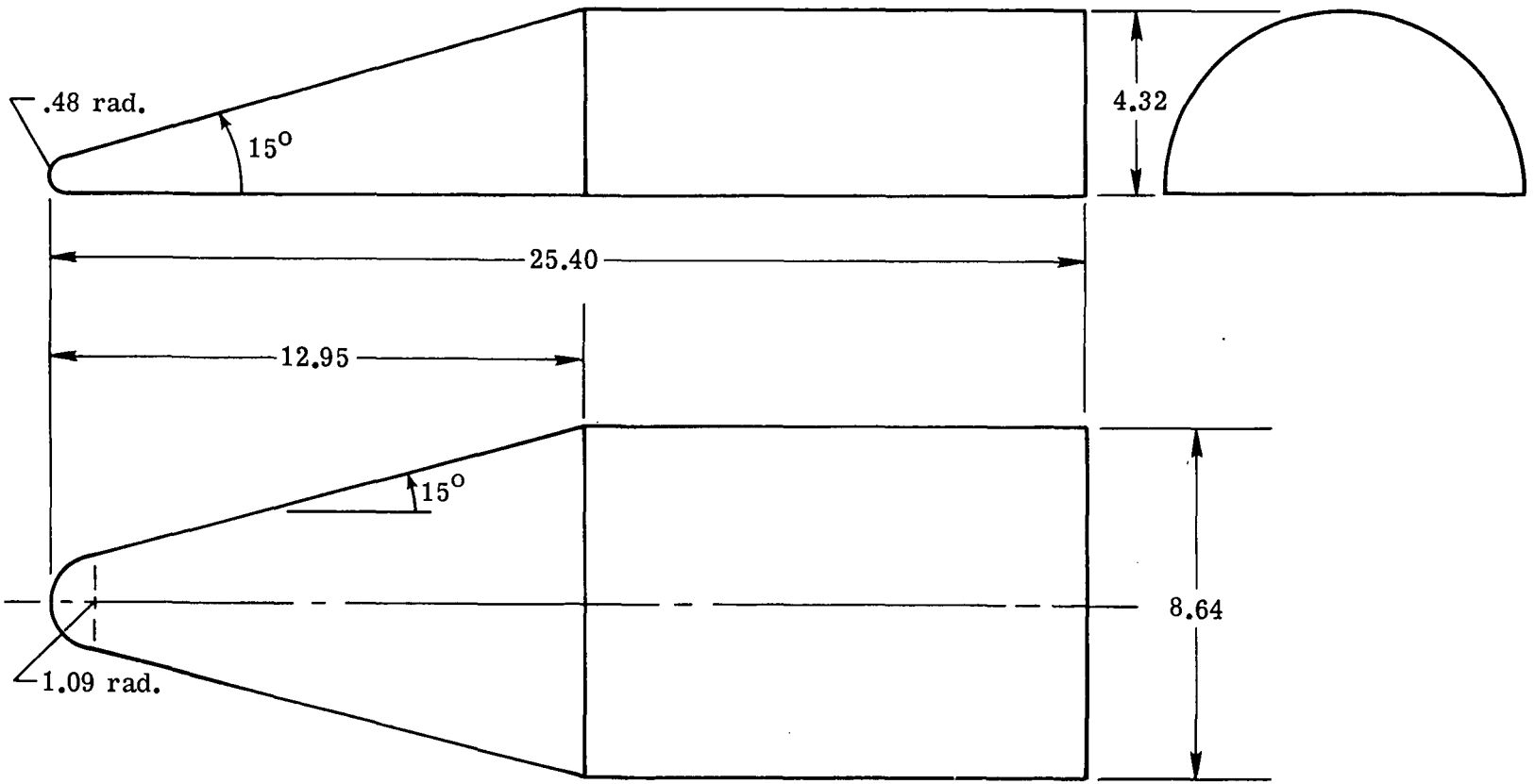

(a) Model 1.

Figure 1.- Drawings of wind-tunnel models. All linear dimensions are in centimeters.

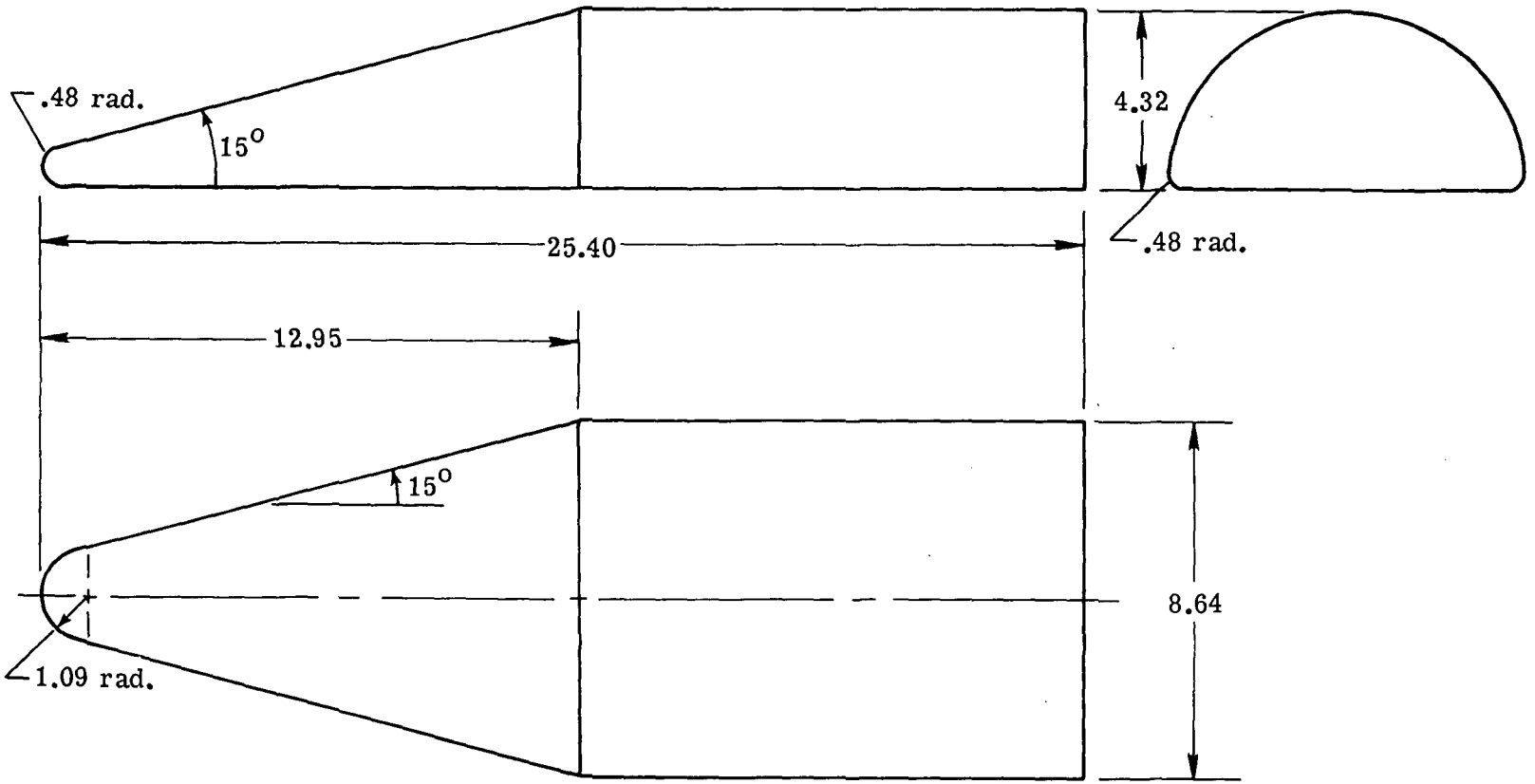

(b) Model 2.

Figure 1.- Continued.

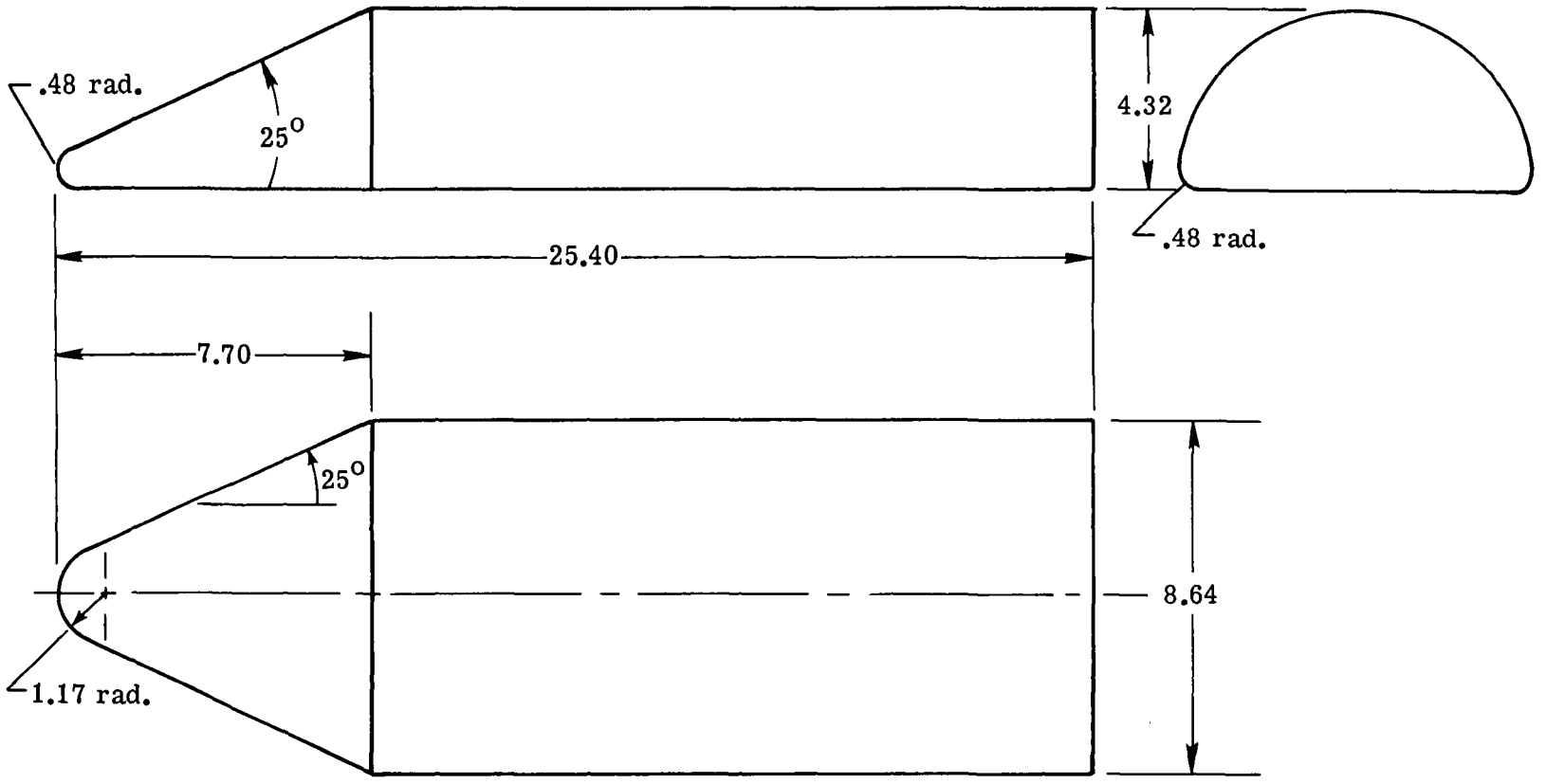

(c) Model 3.

Figure 1.- Continued.

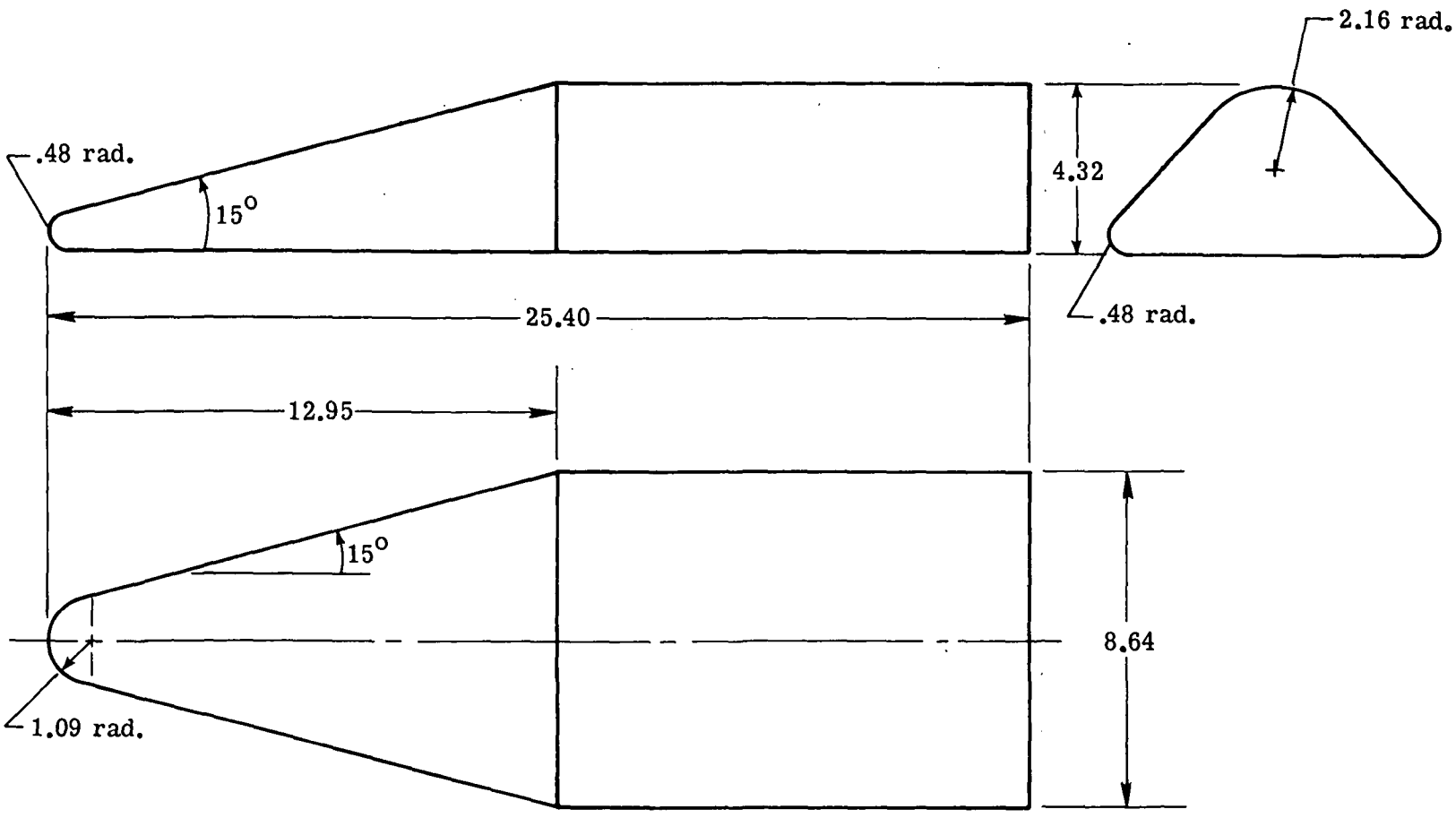

(d) Model 4.

Figure 1.- Continued.

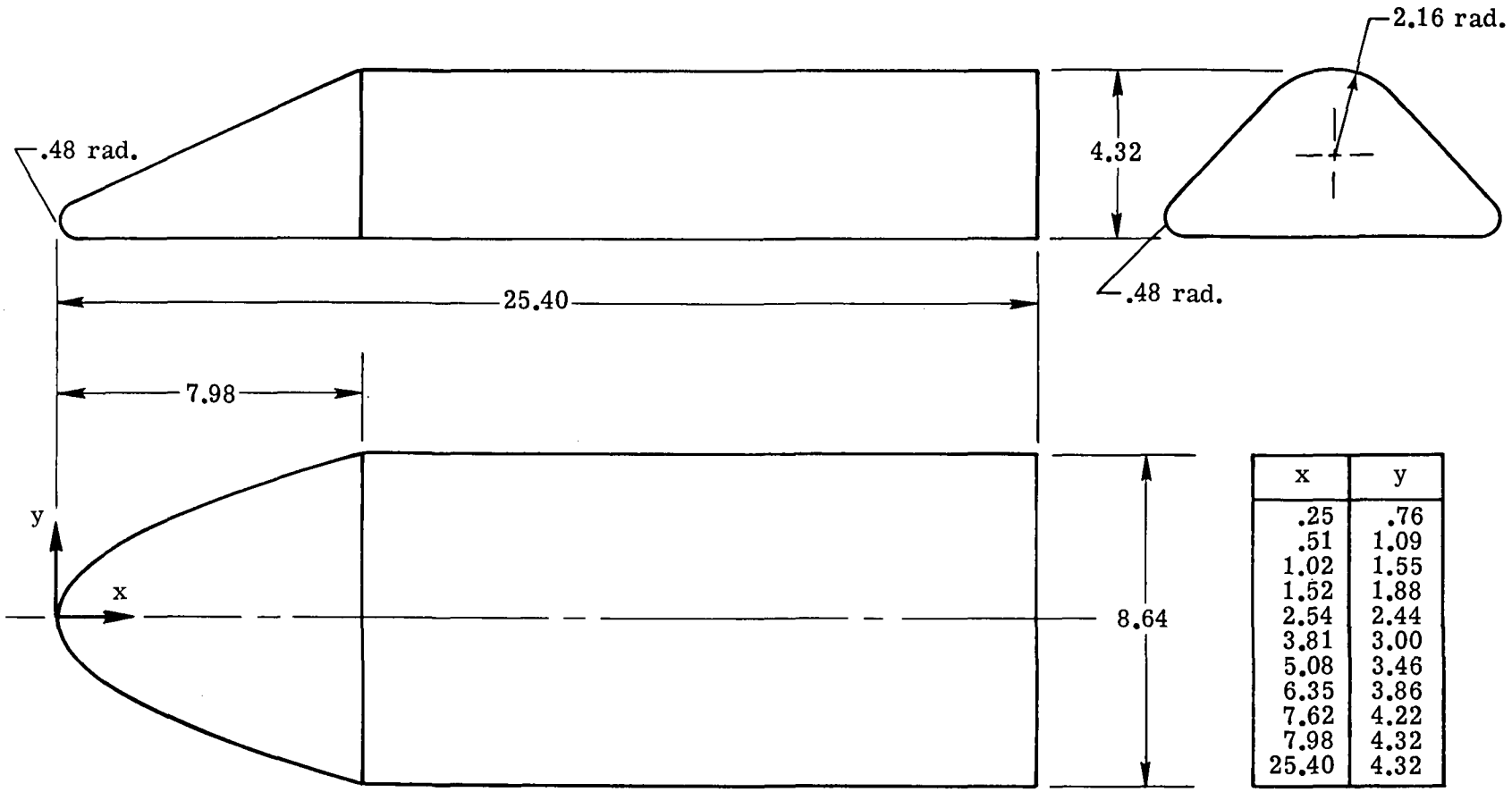

x	y
.25	.76
.51	1.09
1.02	1.55
1.52	1.88
2.54	2.44
3.81	3.00
5.08	3.46
6.35	3.86
7.62	4.22
7.98	4.32
25.40	4.32

(e) Model 5.

Figure 1.- Continued.

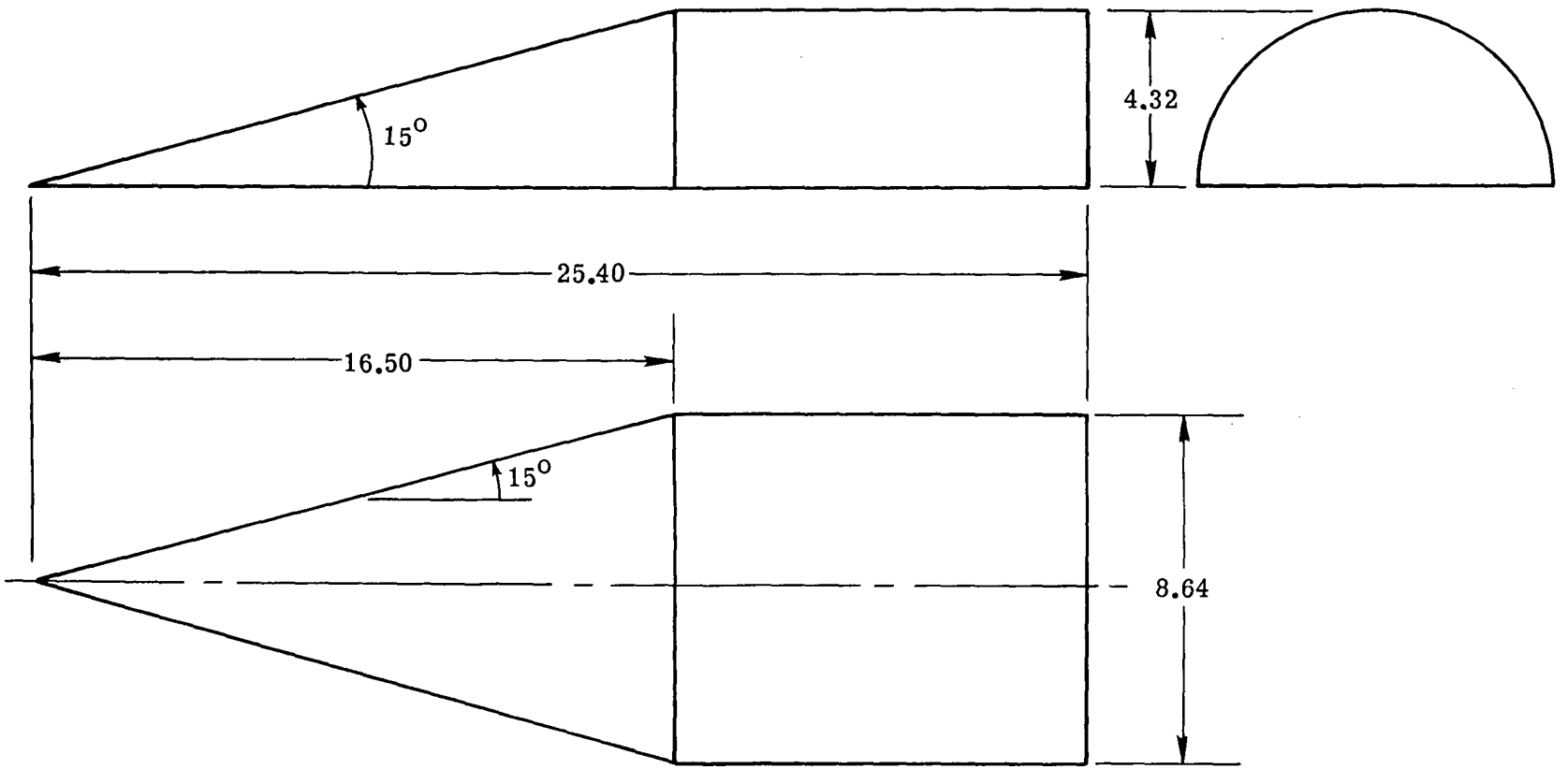

(f) Model 6.

Figure 1.- Concluded.

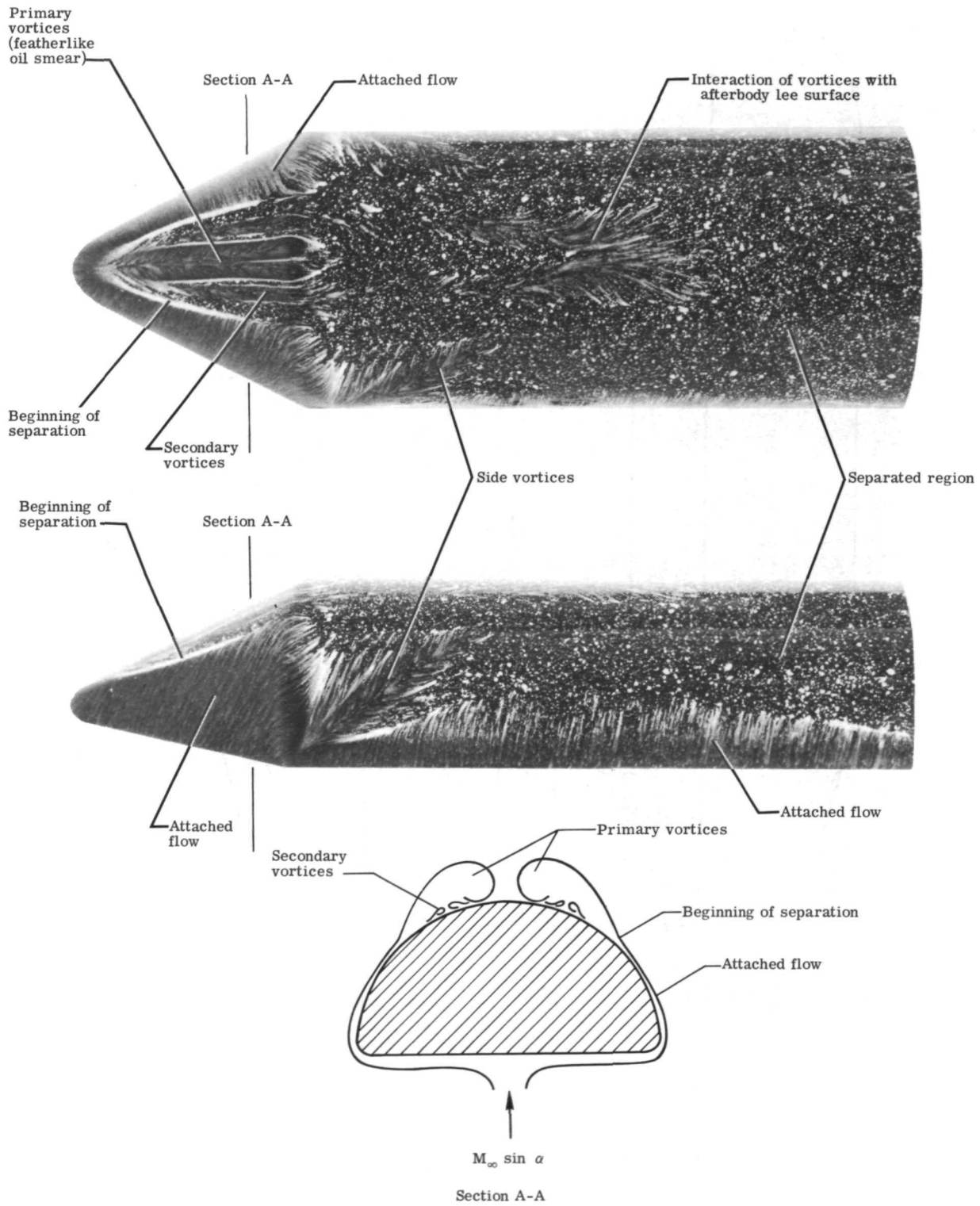

L-73-6879

Figure 2.- Lee-surface characteristics at $\alpha = 40^o$. $M_\infty = 6$; $R_{\infty,L} = 4.34 \times 10^6$.

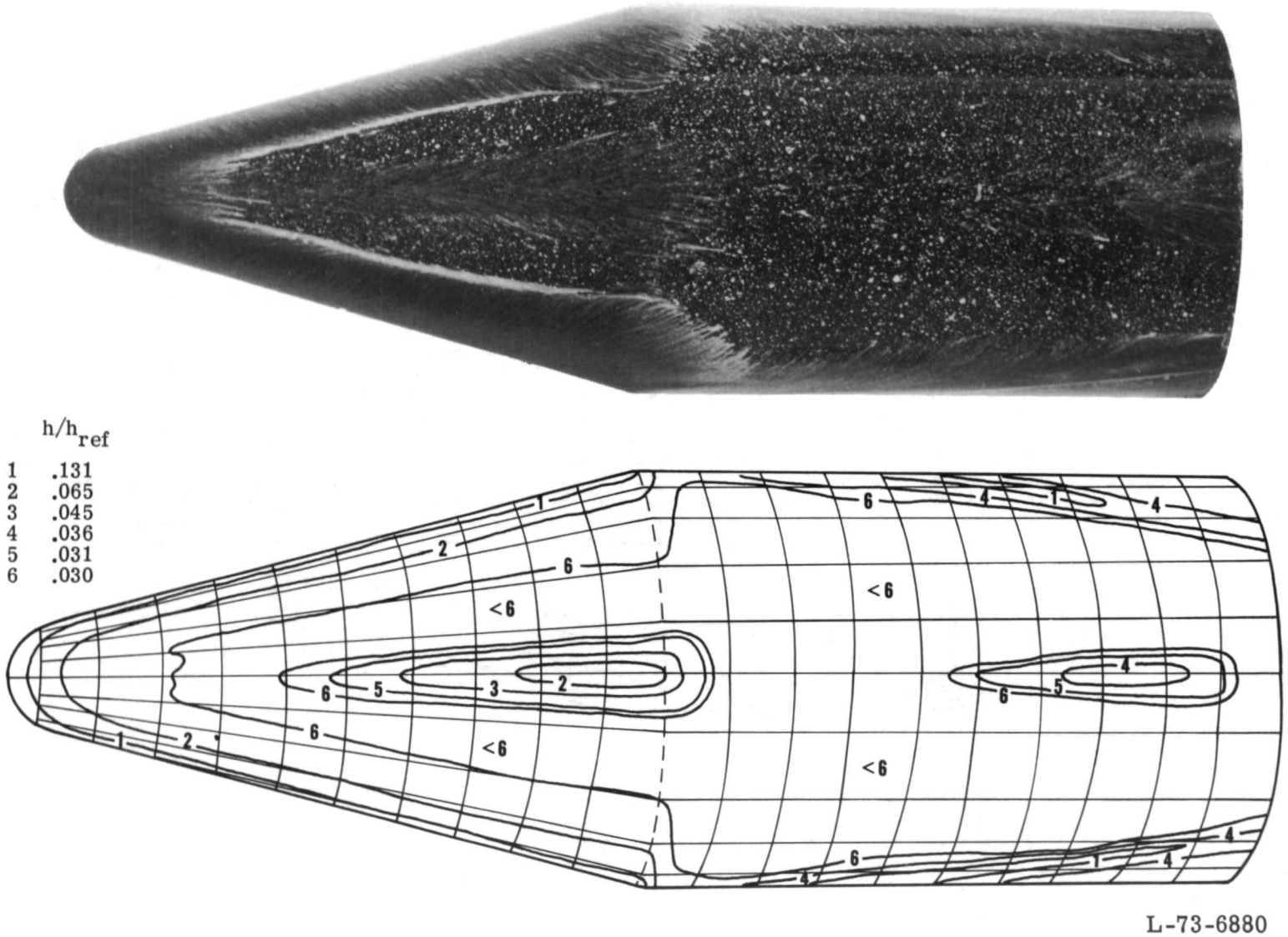

(a) Model 1.

Figure 3.- Heat-transfer and oil-flow distributions at $\alpha = 20^{o}$. $M_{\infty} = 6$; $R_{\infty,L} = 4.34 \times 10^{6}$.

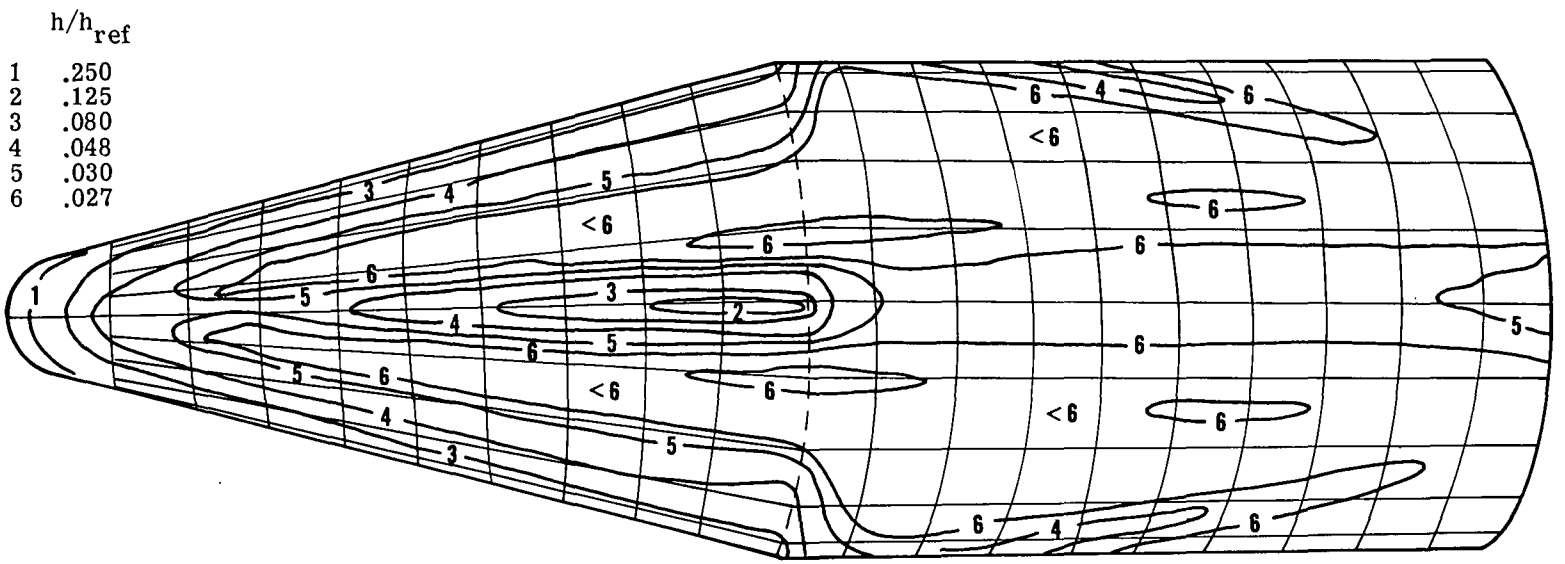

(b) Model 2. (No oil-flow distributions obtained.)

Figure 3.- Continued.

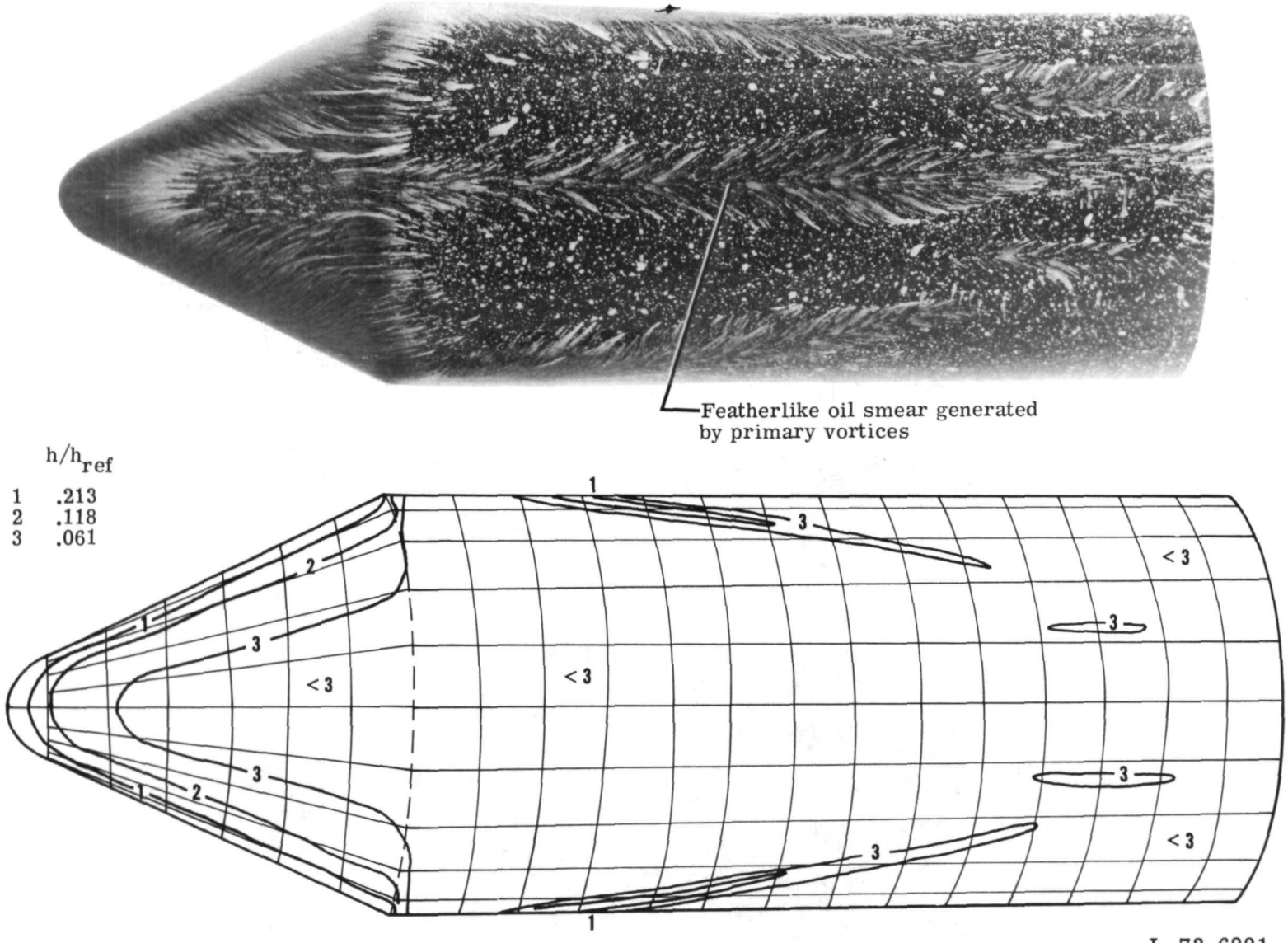

(c) Model 3.

Figure 3.- Continued.

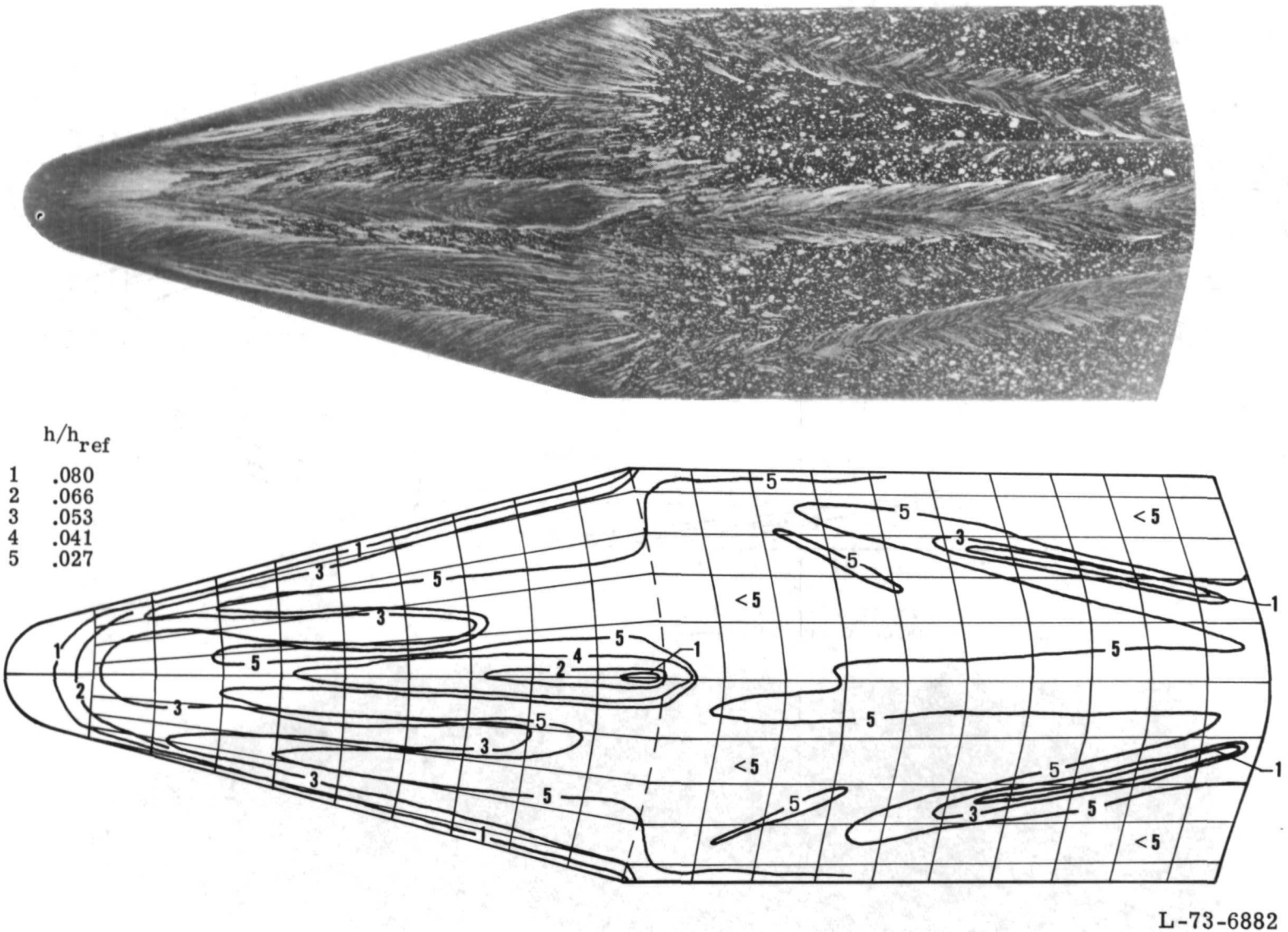

(d) Model 4.

Figure 3.- Continued.

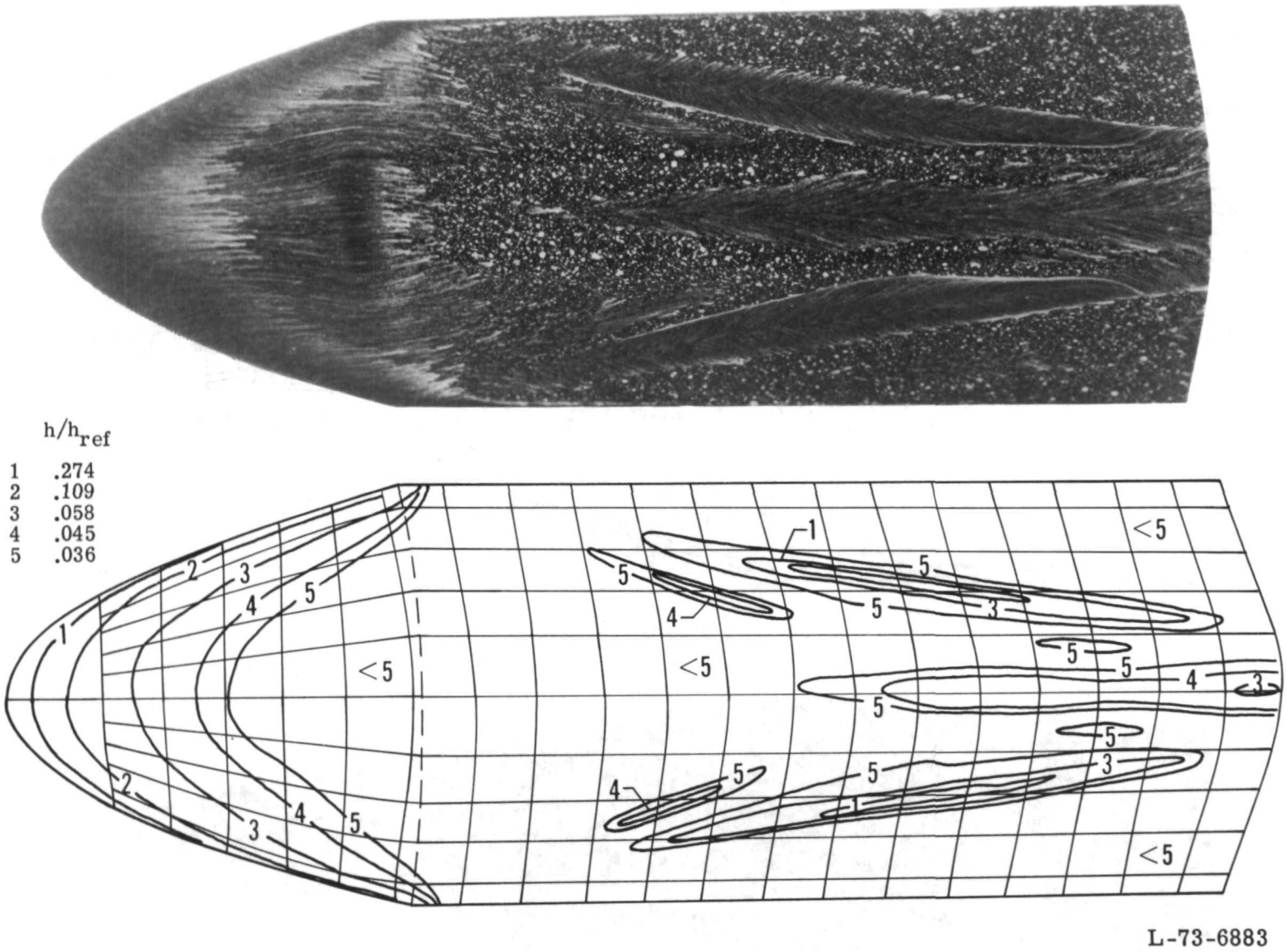

(e) Model 5.

Figure 3.- Continued.

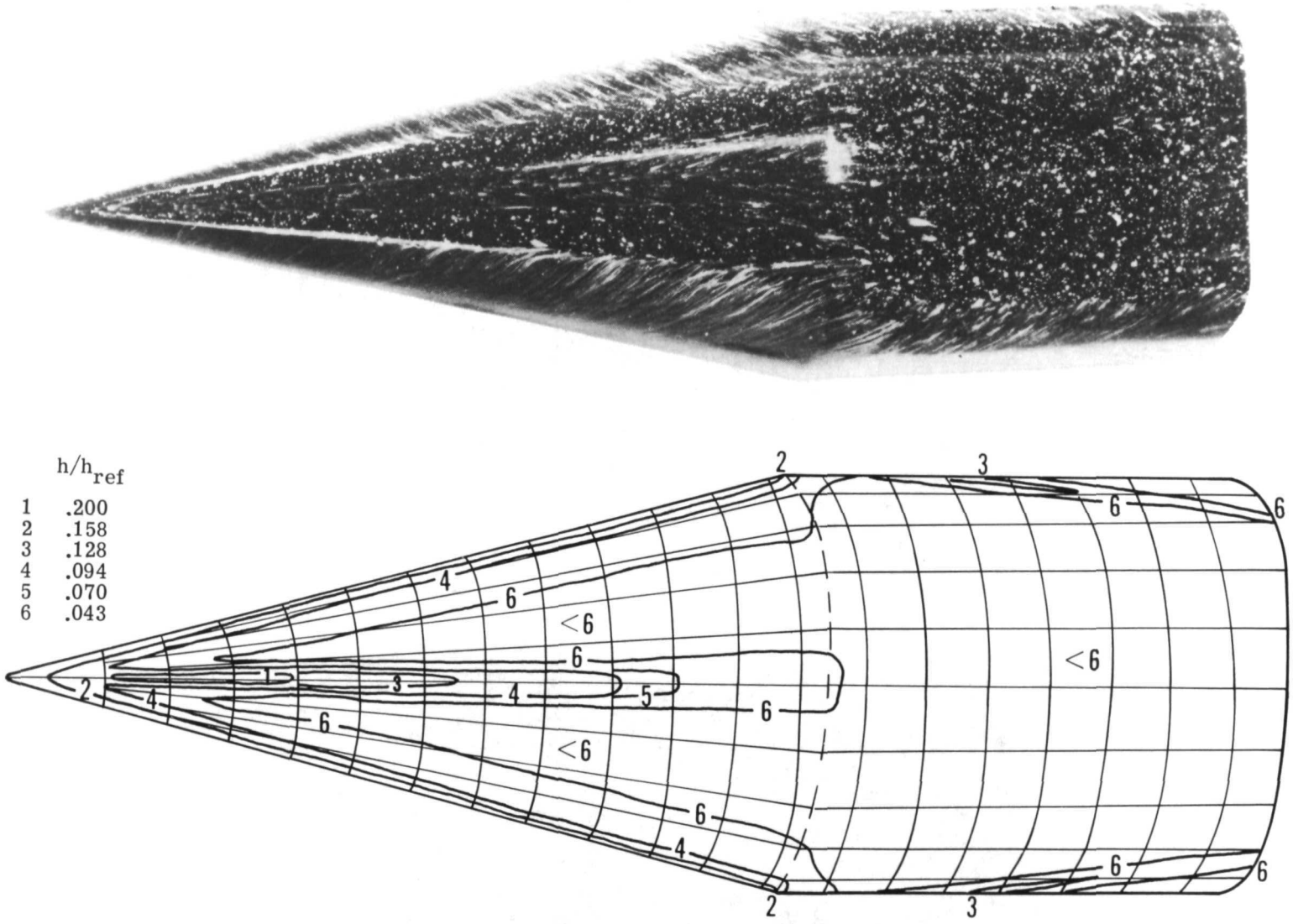

(f) Model 6.

Figure 3.- Concluded.

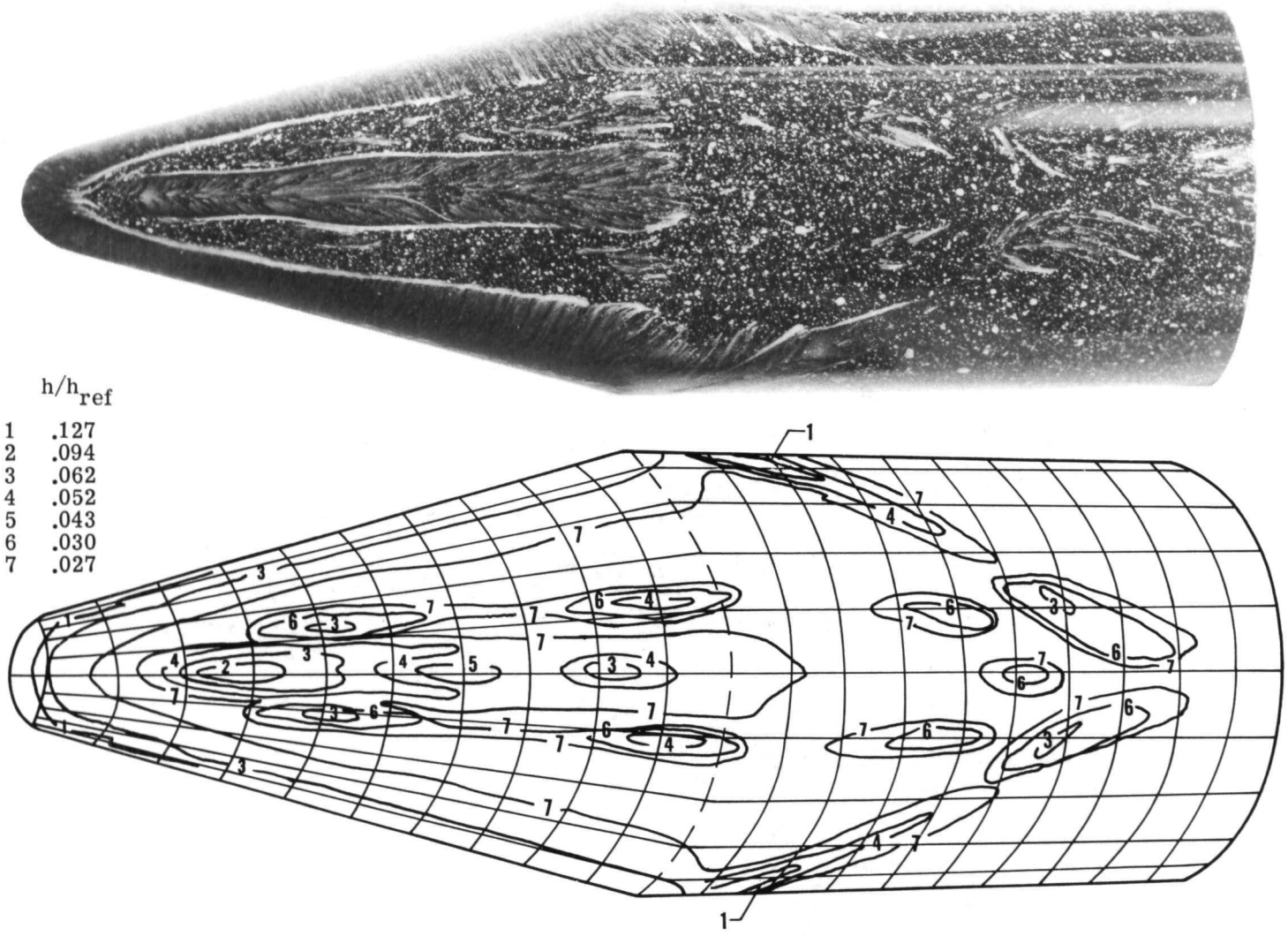

(a) Model 1.

Figure 4.- Heat-transfer and oil-flow distributions at $\alpha = 40^{o}$. $M_{\infty} = 6$; $R_{\infty,L} = 4.34 \times 10^{6}$.

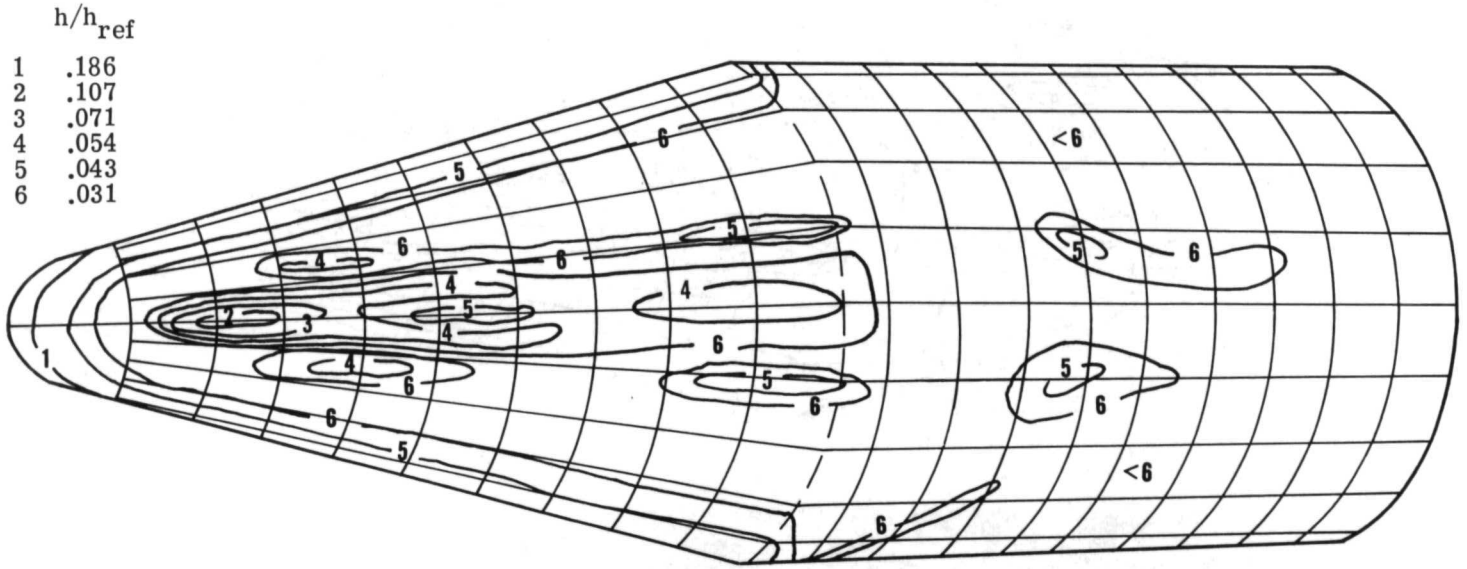

(b) Model 2. (No oil-flow distributions obtained.)

Figure 4.- Continued.

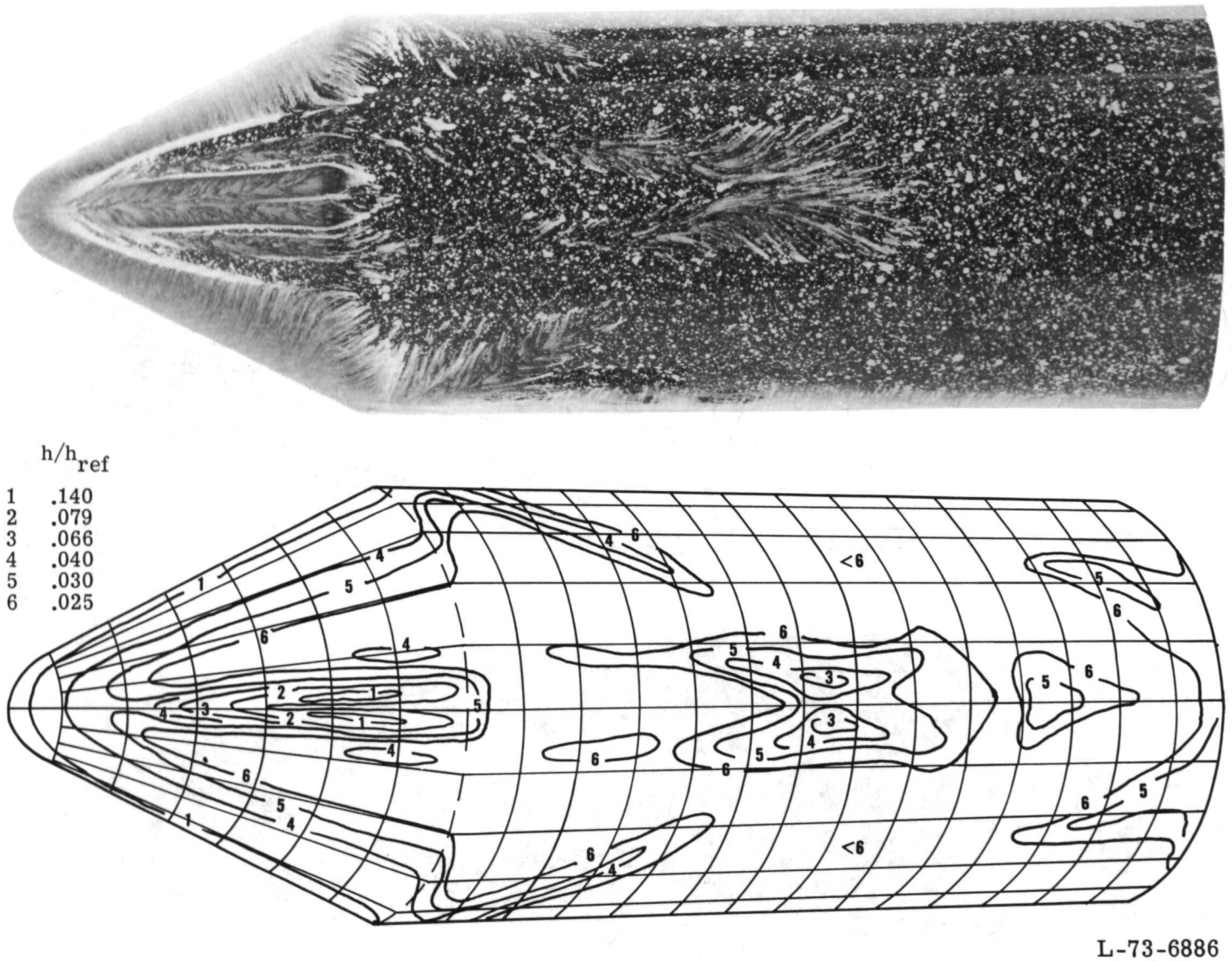

(c) Model 3.

Figure 4.- Continued.

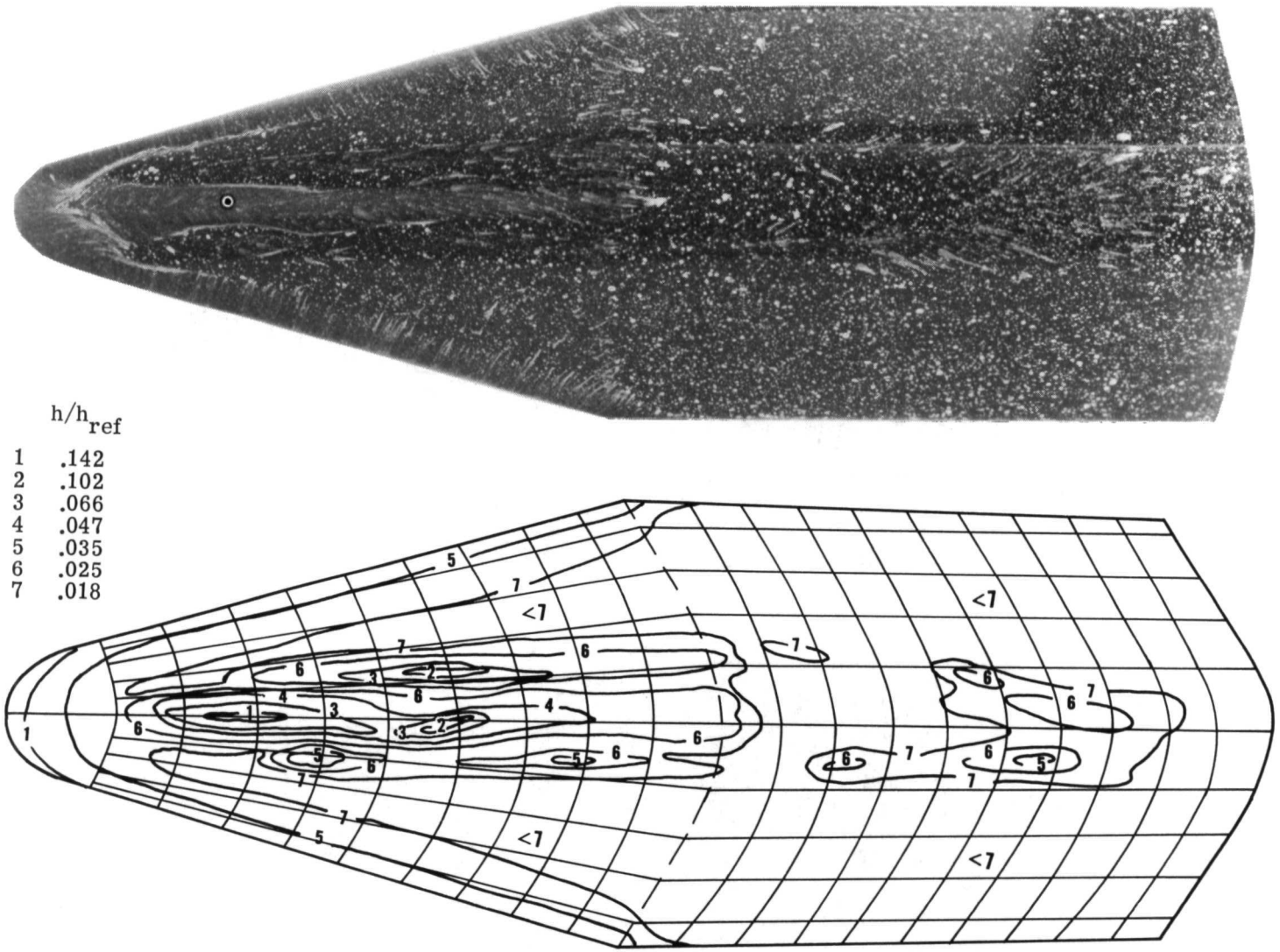

(d) Model 4.

Figure 4.- Continued.

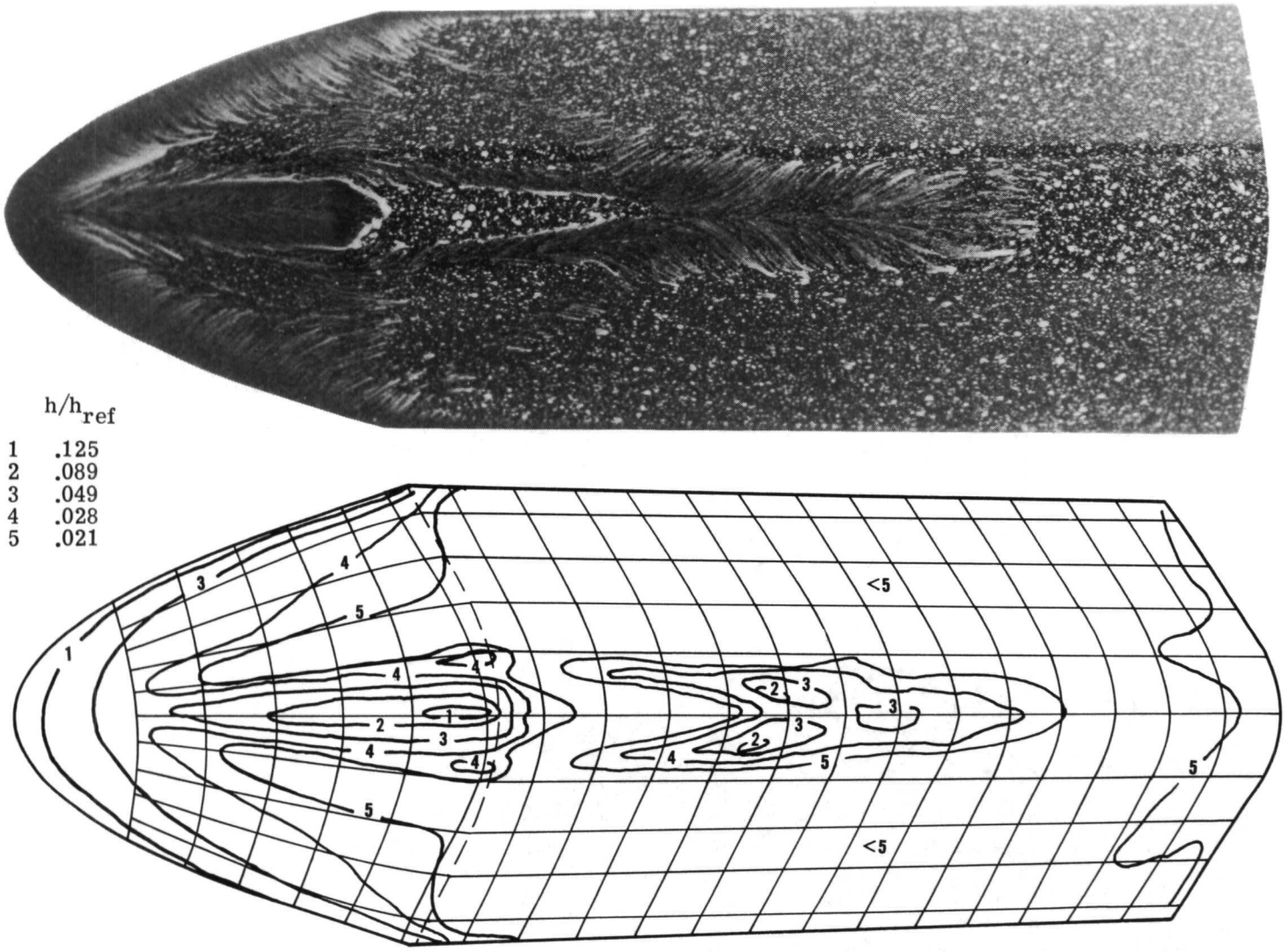

(e) Model 5.

Figure 4.- Continued.

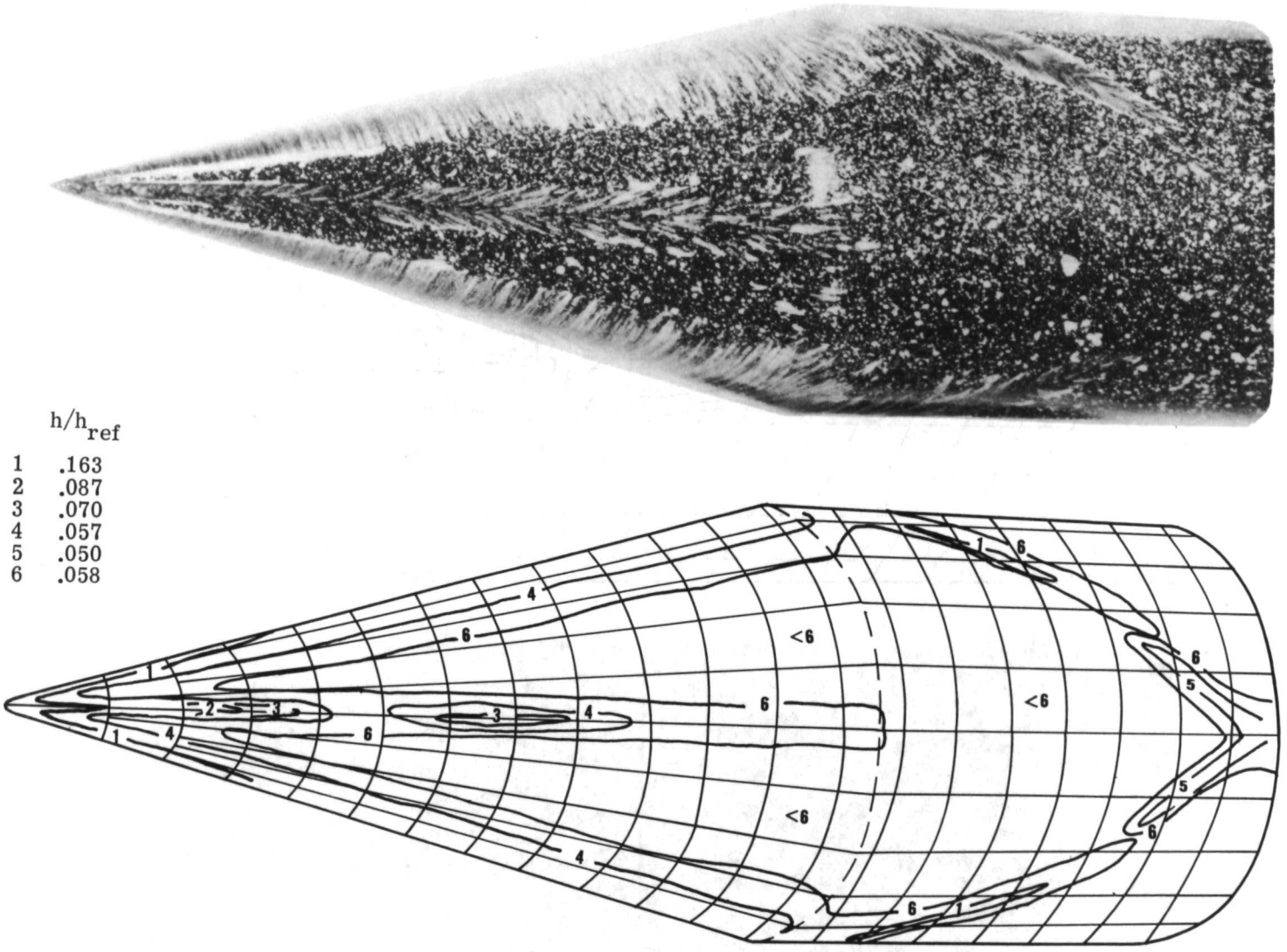

L-73-6889

(f) Model 6.

Figure 4.- Concluded.

NATIONAL AERONAUTICS AND SPACE ADMINISTRATION
WASHINGTON, D.C. 20546

OFFICIAL BUSINESS
PENALTY FOR PRIVATE USE $300

SPECIAL FOURTH-CLASS RATE
BOOK

POSTAGE AND FEES PAID
NATIONAL AERONAUTICS AND
SPACE ADMINISTRATION
451

U.S.MAIL

POSTMASTER: If Undeliverable (Section 158 Postal Manual) Do Not Return

"The aeronautical and space activities of the United States shall be conducted so as to contribute . . . to the expansion of human knowledge of phenomena in the atmosphere and space. The Administration shall provide for the widest practicable and appropriate dissemination of information concerning its activities and the results thereof."

—NATIONAL AERONAUTICS AND SPACE ACT OF 1958

NASA SCIENTIFIC AND TECHNICAL PUBLICATIONS

TECHNICAL REPORTS: Scientific and technical information considered important, complete, and a lasting contribution to existing knowledge.

TECHNICAL NOTES: Information less broad in scope but nevertheless of importance as a contribution to existing knowledge.

TECHNICAL MEMORANDUMS: Information receiving limited distribution because of preliminary data, security classification, or other reasons. Also includes conference proceedings with either limited or unlimited distribution.

CONTRACTOR REPORTS: Scientific and technical information generated under a NASA contract or grant and considered an important contribution to existing knowledge.

TECHNICAL TRANSLATIONS: Information published in a foreign language considered to merit NASA distribution in English.

SPECIAL PUBLICATIONS: Information derived from or of value to NASA activities. Publications include final reports of major projects, monographs, data compilations, handbooks, sourcebooks, and special bibliographies.

TECHNOLOGY UTILIZATION PUBLICATIONS: Information on technology used by NASA that may be of particular interest in commercial and other non-aerospace applications. Publications include Tech Briefs, Technology Utilization Reports and Technology Surveys.

Details on the availability of these publications may be obtained from:

SCIENTIFIC AND TECHNICAL INFORMATION OFFICE

NATIONAL AERONAUTICS AND SPACE ADMINISTRATION

Washington, D.C. 20546